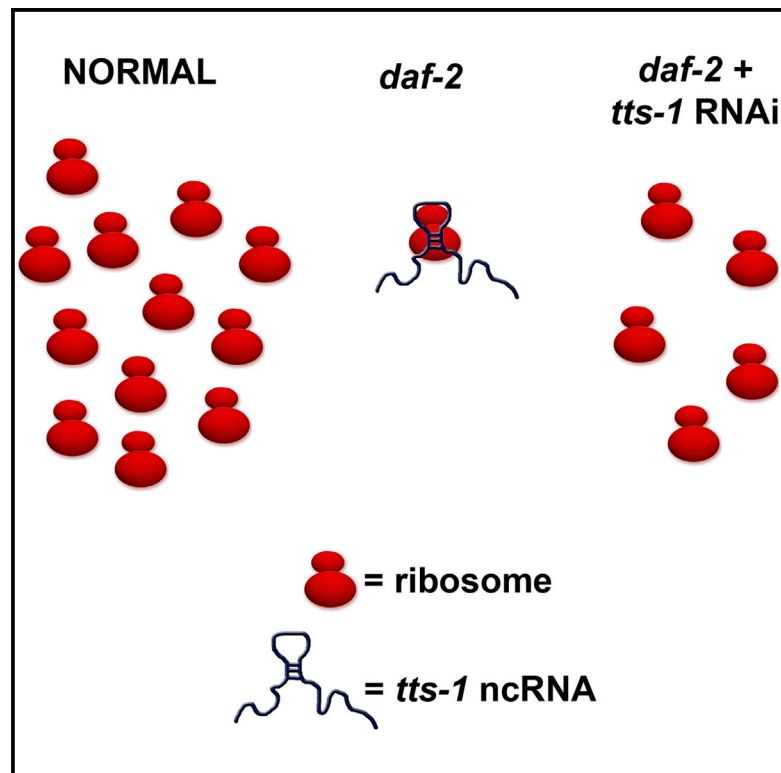# A Long Noncoding RNA on the Ribosome Is Required for Lifespan Extension

Graphical Abstract

Authors

Paul B. Essers, Julie Nonnekens, ...,
Arjan B. Brenkman, Alyson W. MacInnes

Correspondence

a.macinnes@sanquin.nl

In Brief

Essers et al. find a long noncoding RNA, transcribed telomeric sequence 1 (*tts-1*), on ribosomes of *C. elegans* carrying the life-extending *daf-2* insulin receptor mutation as well as the *clk-1* mitochondrial mutant. They then demonstrate that this RNA is required for the life-extension phenotypes and that its depletion results in increasing ribosome levels.

Highlights

- The long noncoding RNA *tts-1* is found on *C. elegans daf-2* mutant ribosomes

- Depletion of *tts-1* restores ribosome levels in *daf-2* mutants

- The extended lifespans of *daf-2* and *clk-1* mutants are dependent on *tts-1*

CrossMark

CellPress

A Long Noncoding RNA on the Ribosome Is Required for Lifespan Extension

Paul B. Essers,[1,4] Julie Nonnekens,[1,4] Yvonne J. Goos,[1,4] Marco C. Betist,[1] Marjon D. Viester,[1] Britt Mossink,[1] Nico Lansu,[1] Hendrik C. Korswagen,[1] Rob Jelier,[2] Arjan B. Brenkman,[3] and Alyson W. MacInnes[1,5,*]

[1]Hubrecht Institute, KNAW and University Medical Center Utrecht, 3584 CT Utrecht, the Netherlands
[2]Centre of Microbial and Plant Genetics, KU Leuven, Kasteelpark Arenberg 20, 3001 Leuven, Belgium
[3]Section Metabolic Diseases, Department of Molecular Cancer Research, Wilhelmina Children's Hospital, University Medical Center Utrecht, 3508 AB Utrecht, the Netherlands
[4]Co-first author
[5]Present address: Department of Hematopoiesis, Sanquin Research and Landsteiner Laboratory, Plesmanlaan 125, 1066 CX Amsterdam, the Netherlands
*Correspondence: a.macinnes@sanquin.nl
http://dx.doi.org/10.1016/j.celrep.2014.12.029

SUMMARY

The biogenesis of ribosomes and their coordination of protein translation consume an enormous amount of cellular energy. As such, it has been established that the inhibition of either process can extend eukaryotic lifespan. Here, we used next-generation sequencing to compare ribosome-associated RNAs from normal strains of *Caenorhabditis elegans* to those carrying the life-extending *daf-2* mutation. We found a long noncoding RNA (lncRNA), transcribed telomeric sequence 1 (*tts-1*), on ribosomes of the *daf-2* mutant. Depleting *tts-1* in *daf-2* mutants increases ribosome levels and significantly shortens their extended lifespan. We find *tts-1* is also required for the longer lifespan of the mitochondrial *clk-1* mutants but not the feeding-defective *eat-2* mutants. In line with this, the *clk-1* mutants express more *tts-1* and fewer ribosomes than the *eat-2* mutants. Our results suggest that the expression of *tts-1* functions in different longevity pathways to reduce ribosome levels in a way that promotes life extension.

INTRODUCTION

The aging of eukaryotes depends on a number of genetic and environmental factors. One of the best-studied pathways controlling lifespan is the highly conserved insulin/IGF-1 pathway. Within this pathway is the well-known *daf-2* mutation in the insulin receptor, which in *Caenorhabditis elegans* results in a 2- to 3-fold extension of life (Kenyon, 2010). This increase in insulin/IGF-1-mediated lifespan is dependent on the Forkhead transcription factor DAF-16 inducing the expression of a number of stress-resistance genes as well as an increase of the cellular self-digestion and recycling process of autophagy (Kenyon et al., 1993; McElwee et al., 2003; Meléndez et al., 2003; Murphy et al., 2003). Other longevity pathways mechanistically distinct from insulin signaling include the mutation of mitochondrial path-

ways controlling respiration and physiological timing, the inhibition of protein translation through reducing ribosomal proteins or inhibition of the mammalian target of rapamycin (mTOR) pathway, and dietary restriction that is also thought to function through mTOR (Blagosklonny, 2010; Hansen et al., 2007; Jonassen et al., 1998; Kenyon, 2010; Lakowski and Hekimi, 1996, 1998; Wong et al., 1995). The loss of ribosome elements such as ribosomal proteins in the mitochondria leads to decreased respiration and increased lifespan in *C. elegans*, while in *S. cerevisiae*, the depletion of ribosomal proteins in the cytoplasm also increases lifespan (Houtkooper et al., 2013; Steffen et al., 2008). Taken together, the data indicate that the reduction of ribosome levels and/or the deceleration of protein translation are ways to extend lifespan.

We and others recently determined that the *C. elegans* proteome of the *daf-2(e1370)* mutant (hereafter referred to as *daf-2*) reveals a dramatic reduction of ribosomal proteins, mRNA processing components, and protein metabolism factors compared to N2 wild-types (Depuydt et al., 2014; Stout et al., 2013). In turn, both studies using different experimental approaches found that the rate at which de novo proteins are synthesized is significantly reduced in *daf-2* mutant cells. However, each study also found that the total amount of protein in the *daf-2* mutants remains equivalent to wild-types, likely reflecting concurrent reductions in protein metabolism (Depuydt et al., 2014; Stout et al., 2013).

RESULTS

We hypothesized that the *daf-2* reduction of protein synthesis would be reflected by changes in ribosome-associated RNAs. In order to compare these RNA subsets, we took a nonbiased approach by performing next-generation sequencing on the RNAs isolated from the monosomal or polysomal fractions (hereafter referred to as "ribosomal") of N2, *daf-2*, and *daf-2;daf-16* strains normalized to total protein amounts and separated over sucrose density gradients (experimental setup shown in Figure S1A). The expected reduction of the ribosome profile peaks specifically in the *daf-2* mutants compared to wild-type levels was consistent with our previous findings (Stout et al., 2013). Figure S1B illustrates the relative proportion of different subsets of
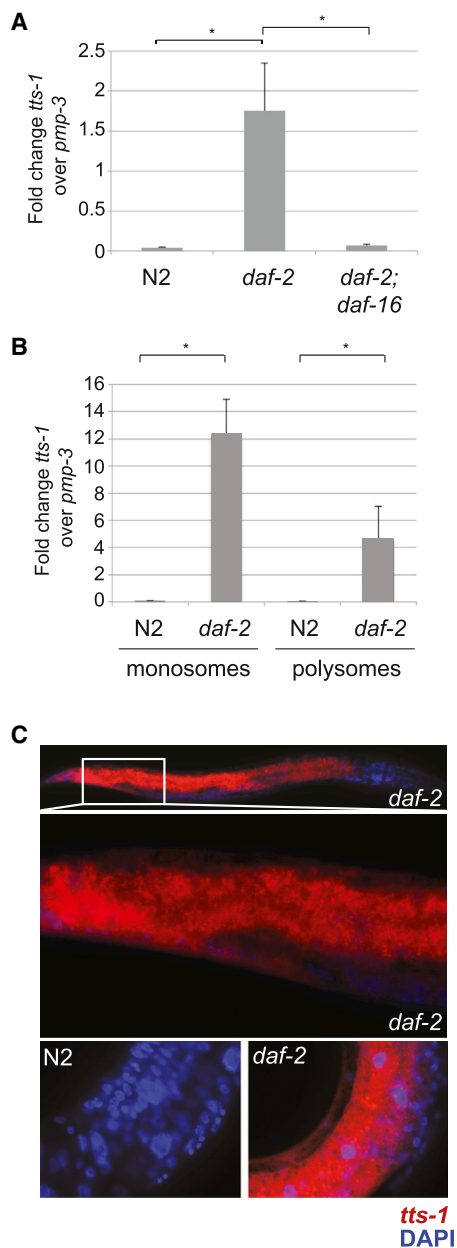
Figure 1. tts-1 lncRNA Expression Is High in the Ribosomal Fractions of daf-2 Mutants

(A) qPCR analysis of tts-1 levels compared to the pmp-3 housekeeping gene in total RNA isolated from N2, daf-2, and daf-2;daf-16 strains. The expression of pmp-3 is set to 1.

(B) qPCR analysis of tts-1 expression compared to pmp-3 RNA isolated from monosomal and polysomal fractions of N2 and daf-2 strains. The expression of pmp-3 is set to 1.
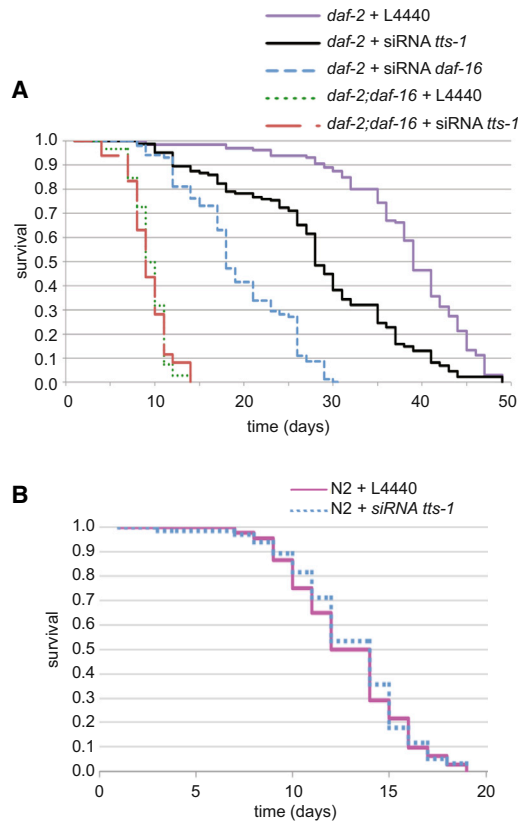
(C) Fluorescent in situ hybridization of tts-1 probes (red) in N2 or daf-2 mutants. The white box in the top panel is enlarged in the panel beneath. DAPI (blue) is used for nuclear staining. *p < 0.01. See also Figure S1.

strains largely code for proteins important for biological processes such as growth, development, the cell cycle, and reproduction, while the same fractions of the daf-2 mutants reveal mRNAs that largely code for proteins involved in aging and stress response. Gene Ontology (GO) analysis of gene functions using Database Annotation, Visualization, and Integrated Discovery (DAVID) in Figure S1C confirmed these biological functions to be consistent with other studies measuring transcriptional changes in the daf-2 mutant (Halaschek-Wiener et al., 2005; Murphy, 2006).

In addition to the differential enrichment of many mRNAs on daf-2 ribosomes, we also found a long noncoding RNA (lncRNA), transcribed telomeric sequence 1 (tts-1), highly expressed in ribosomal fractions of daf-2 cells, but not in those of N2 or daf-2;daf-16. The tts-1 lncRNA is transcribed to two different isoforms of 711 or 659 bp long from a gene found on chromosome X that is not conserved in any other species and has almost no homology with other C. elegans genes. The G/C content of the tts-1 transcript is very low, calculated to be 34% for the total length of the transcript and dropping to less than 15% at the final 150 bp of the 3′ end. A low-affinity cyclic-AMP responsive element (TGATGTCA) lies 728 nt upstream of the tts-1 transcription start site. Figure S1D illustrates the location of the RNA-seqencing mapped read densities with an Integrative Genomics Viewer (Robinson et al., 2011). Serial analysis of gene expression (SAGE) previously found that compared to wild-type strains, tts-1 is one of the most upregulated transcripts in the daf-2 mutants as well as in the developmentally arrested and longer-lived C. elegans in dauer formation (a type of stasis resulting from unfavorable environments that permits survival under harsh conditions) (Halaschek-Wiener et al., 2005; Jones et al., 2001). The expression of tts-1 is also significantly upregulated in C. elegans subject to attack by Gram-positive bacterial pathogens, a situation that slows the growth and increases constipation of the worms (O'Rourke et al., 2006). However, the function of the tts-1 lncRNA and its role in the longevity and immunity programs of C. elegans are, to date, entirely unknown.
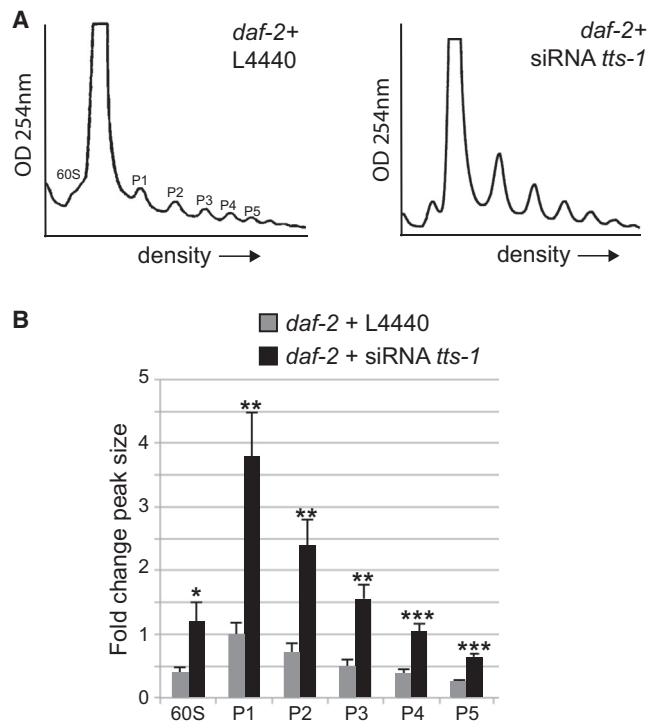
We first validated the increase of tts-1 expression in daf-2 mutants compared to the levels in N2s and daf-2;daf-16 mutants using qPCR analysis of cDNA generated from isolated total RNA. The results of tts-1 expression are shown compared to expression of the pmp-3 housekeeping gene. This gene has been previously validated as an optimal reference gene for qPCR in C. elegans (Zhang et al., 2012) and remains unchanged in our next-generation sequencing data sets. Figure 1A shows that with the expression of pmp-3 set to 1, there is almost no detectable tts-1 expression in N2s or daf-2;daf-16 mutants. This is compared to an approximately 2-fold increase of expression of tts-1 over pmp-3 in the daf-2 mutants, confirming previous reports of high tts-1 expression in these mutants and also suggesting this expression is at least partly daf-16 dependent. Further qPCR results comparing the levels of tts-1 on N2 and daf-2 monosomes and polysomes reveal that compared to pmp-3, tts-1 is enriched over 12-fold in the daf-2 monosomal fraction and over 4-fold in the daf-2 polysomal fraction, with again almost no detectable tts-1 found in either fraction of the N2 strain (Figure 1B). These data suggest that tts-1 is not only expressed at much higher levels in daf-2 mutants but also preferentially

RNAs that we found in the ribosomal fractions of N2, daf-2, and daf-2;daf-16 strains. Tables S1 and S2 reveal that the mRNAs found in the ribosomal fractions of the N2 and daf-2;daf-16

Figure 2. *tts-1* Depletion Decreases the Lifespan of *daf-2* Mutants

(A) Survival curve of *daf-2* or *daf-2;daf-16* mutants fed bacteria transformed with empty L4440, *tts-1* siRNA, or an siRNA construct against *daf-16* as a positive control. See also Figure S2.

(B) Survival curve of N2 worms fed bacteria expressing the empty L4440 vector or *tts-1* siRNA.

Figure 3. Depletion of *tts-1* Restores Ribosome Levels in *daf-2* Mutants

(A) Representative polysome profiles of *daf-2* mutants fed bacteria transformed with the empty L4440 vector (A) or L4440 expressing *tts-1* siRNA when lysate is normalized to total protein levels (B). The peak numbers are indicated (P1–P5).

(B) Quantification of polysome peak sizes. The fold change is represented compared to P1 of the *daf-2* controls. *p < 0.05, **p < 0.02, ***p < 0.01. See also Figure S3.

enriched on ribosomes. Fluorescent in situ hybridization analysis (FISH) with 11 different probes against *tts-1* confirmed the substantially higher expression of *tts-1* in *daf-2* mutants compared to N2 (Figure 1C). Moreover, it reveals that *tts-1* is uniformly expressed in the cytoplasm and nuclei of cells in the intestine of the *daf-2* mutant, which is in line with the prominent role of the *C. elegans* intestine in the regulation of insulin/IGF-1 lifespan (Libina et al., 2003). To confirm that *tts-1* is in fact ribosome bound and not merely contaminating the polysomal fractions of the sucrose gradients, we measured levels of *tts-1* in the polysomal fractions of untreated *daf-2* mutants compared to those treated with puromycin. The puromycin-induced dissociation of polysomes is confirmed by profiles revealing a reduction of polysome peaks and a widening of the monosome peak in Figure S1E. This dissociation of polysomes results in a reduction of both *pmp-3* and *tts-1* levels in the polysomal fraction, indicating that the expression of *tts-1* in the polysomal fractions is not merely a contaminant (Figure S1F).

To understand the function of the *tts-1* lncRNA in the context of lifespan extension, we designed a double-stranded small interfering RNA (siRNA) construct against *tts-1* in the L4440 vector that we expressed in HT115 *E. coli* and then fed to the worms.

Compared to *daf-2* mutants fed bacteria expressing the empty L4440 vector, the bacteria expressing the *tts-1* siRNA were successful at reducing the levels of *tts-1* in *daf-2* mutants by over 90% (Figure S2A). This siRNA of *tts-1* significantly shortened the extended lifespan of the *daf-2* mutants (Figures 2A and S2B). Importantly, as opposed to inducing toxicity, *tts-1* is regulating *daf-2* lifespan specifically, as neither wild-type nor *daf-2;daf-16* nematodes reveal any changes in lifespan upon exposure to the *tts-1* siRNA (Figures 2A and 2B). BLAST results of the siRNA sequence revealed no significant homology between the construct and any other gene in the *C. elegans* genome except for *tts-1* itself, suggesting a low probability of any off-target effect of the siRNA that may negatively affect *daf-2* lifespan (Kamath et al., 2001, 2003). These results reveal a necessary role of *tts-1* in the extension of the *daf-2* mutant lifespan.

We next examined the effect of *tts-1* depletion on the polysome profiles of *daf-2* mutants normalizing the lysate on the gradients to total protein levels. Consistent with what we previously reported (Stout et al., 2013), the profiles of the *daf-2* mutants reveal low levels of ribosomes (Figure 3A). These results are also in line with the reduction of the total number of ribosomal proteins that both proteomic studies of the *daf-2* mutants revealed earlier (Depuydt et al., 2014; Stout et al., 2013). We found

A

B

clk-1 L4440
clk-1 siRNA tts-1

C

eat-2 L4440
eat-2 siRNA tts-1
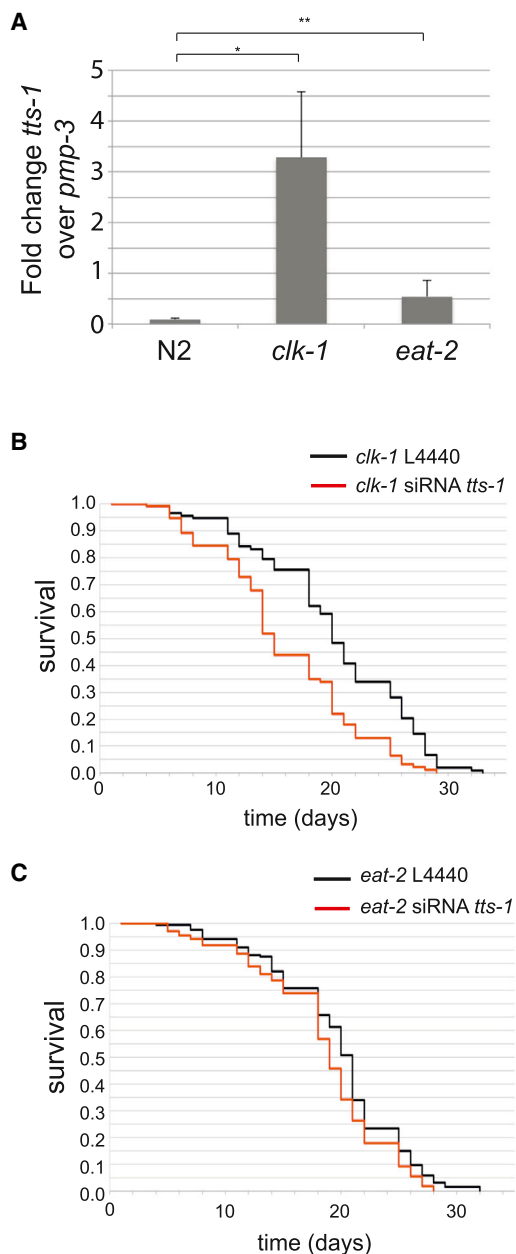
Figure 4. The Effects of *tts-1* Depletion on *clk-1* and *eat-2* Mutant Lifespans

(A) qPCR analysis of *tts-1* expression in *clk-1* and *eat-2* mutants compared to *pmp-3* expression. The expression of *pmp-3* is set to 1.

(B) Longevity curve of *clk-1* mutants fed bacteria expressing empty L4440 vector or L4440 expressing *tts-1* siRNA.

(C) Longevity curve of *eat-2* mutants fed bacteria expressing empty L4440 vector or L4440 expressing *tts-1* siRNA.

*p < 0.01, **p < 0.02. See also Figure S4.

that knocking down the expression of *tts-1* in the *daf-2* mutants results in the polysome peak sizes returning to more wild-type levels, suggesting an increase of ribosome levels (Figures 3B and 3C). In order to evaluate if *tts-1* loss shifted the location of ribosomes from polysomal to nonpolysomal fractions in the den-

sity gradient, which would give an indication about the overall level of protein translation, we then normalized the lysates to cytoplasmic rRNA levels. Here, we detect no difference in the polysome peak sizes (Figure S3A). Moreover, we do not observe any differences in the area under the curves of the polysomal compared to the nonpolysomal fractions (Figure S3B). Taken together, these data suggest that while *tts-1* loss in the *daf-2* mutants increases ribosome levels, it does not affect the overall rate at which these ribosomes translate protein.

In order to assess the stoichiometry of the *tts-1* lncRNA relative to the number of ribosomes, we isolated monosomal RNA from *daf-2* mutants and compared the expression of *tts-1* to 18S rRNA by qPCR analysis. We calculated that for every *tts-1* transcript in the monosomal fraction, there are 116,000 ± 10,000 (n = 3) 18S rRNA transcripts. This suggests that while *tts-1* may be highly expressed in the *daf-2* mutants, it is not acting simply to compete with all other mRNAs for occupancy on the ribosome.

We next asked if the increase of *tts-1* expression and reduction of ribosomes is unique to the insulin/IGF-1 longevity pathway. For these experiments, we used *clk-1(qm30)* mutants (which carry a mitochondrial pathway mutation that reduces respiration and decreases ubiquinone biosynthesis) and *eat-2(ad465)* mutants (models of dietary restriction with impaired pharynxes and defective feeding behavior) (Jonassen et al., 1998; Lakowski and Hekimi, 1996, 1998; Wong et al., 1995). Both of these mutants have an established longer lifespan (Lakowski and Hekimi, 1996, 1998). qPCR analysis relative to *pmp-3* expression on the total RNA isolated from these mutants reveals an increase of *tts-1* expression in both strains compared to N2, with much higher levels of *tts-1* found in the *clk-1* mutants compared to *eat-2* (Figure 4A). Correlating with these results, the profiles of both mutants compared to N2 strains reveal a far more dramatic reduction of ribosome levels in the *clk-1* mutants (Figures S4A and S4B). Further in line with this, we find that the depletion of *tts-1* in the *clk-1* mutants results in a substantial shortening of their longer lifespan (p < 0.0001) and a marginal yet not nearly as significant shortening of the *eat-2* mutant lifespan (p = 0.02) (Figures 4B and 4C). The difference between the effects of *tts-1* depletion on the lifespans of the *clk-1* (and the *daf-2*) versus the *eat-2* mutants moreover supports the specificity of the RNAi and suggests that the changes in lifespan are not due to off-target effects. All of the controls and statistical analysis for this assay are shown in Figures S4C and S4D.

Although we did attempt to construct a *C. elegans* strain overexpressing *tts-1* in the N2 genetic background, we were unsuccessful in establishing an integrated line that expressed *tts-1* at physiological levels or that did not reveal toxicity (data not shown). Thus, whether *tts-1* is sufficient to extend lifespan remains to be determined.

DISCUSSION

Long noncoding RNAs were until recently thought to exist and function predominantly in the nucleus. It is now fast becoming realized that they effusively associate with cytosolic ribosomes (van Heesch et al., 2014; Wilson and Masel, 2011). Several functions for short noncoding RNAs (<20 bp) bound to ribosomes

have been described, such as those that derive from both mRNAs and tRNAs and function as stress-induced inhibitors of protein translation (Ivanov et al., 2011; Pircher et al., 2014; Sobala and Hutvagner, 2013). Also recently a function for the ribosome-bound long intergenic noncoding RNA p21 (lincRNA-p21) was found to selectively repress the translation of *JUNB* and *CTNNB1* mRNAs (Yoon et al., 2012). It is thus becoming clear that ncRNAs, both short and long, are playing roles in protein translation that are only beginning to be fully appreciated.

We are unable to definitively state that the *tts-1* lncRNA does not code for protein. We do not find any protein sequences in http://www.wormbase.org or the NCBI database that corresponded to potential open reading frames of *tts-1.* Moreover, we do not detect any corresponding peptides in our proteomics study (Stout et al., 2013). It may of course be that any synthesized peptides are too small in size or short in half-life to be detected by current proteomic methods. Thus, it remains an open question as to the protein-coding potential of lncRNAs on the ribosome, reflected by a number of conflicting recent reports (Guttman et al., 2013; Niazi and Valadkhan, 2012; Smith et al., 2014).

The strong effect of *tts-1* depletion on the longevity phenotype of the *daf-2* and *clk-1* mutants, but not the *eat-2* mutants, is curious, especially given that the *clk-1* mutation is known to be *daf-16* independent (Lakowski and Hekimi, 1996). It is known that AAK-2, the *C. elegans* homolog of AMP-activated kinase subunit α, functions as a sensor of energy levels and is activated in conditions with high AMP:ATP ratios (Apfeld et al., 2004). Both *clk-1*- and *daf-2*-extended lifespans are dependent on AAK-2 in a pathway that is not shared by *eat-2* (Curtis et al., 2006). Recently, it was shown that CRTC-1 (the sole *C. elegans* cyclic-AMP response element binding protein [CREB]-regulated transcriptional coactivator) interacts with the CREB homolog-1 transcription factor (CRH-1) and is directly activated by AAK-2 (Mair et al., 2011). As mentioned previously, a low-affinity cyclic-AMP responsive element lies 728 nt upstream of the *tts-1* transcription start site. It is therefore possible that AMP:ATP levels are a driver of *tts-1* transcription, which would also account for the high *tts-1* expression in animals attacked by Gram-positive pathogens as they respond to the invasive stress and increase the AMP:ATP ratio (Hardie, 2011).

The precise mechanism of the *tts-1* lncRNA remains to be determined. One intriguing possibility is that it is specifically regulating the translation of ribosomal protein mRNAs. Supporting this notion is the observation that despite the marked reduction of ribosomal proteins in the *daf-2* mutant proteome, expression levels of ribosomal protein mRNAs in the *daf-2* mutants are actually higher than in wild-types (Depuydt et al., 2014; Halaschek-Wiener et al., 2005). This suggests that a specific block of ribosomal protein gene expression at the level of translation is imposed in mutants undergoing lifespan extension, and we believe this will be an interesting area of future study.

In sum, we propose that the *tts-1* lncRNA is able to reduce ribosome levels in a manner that is necessary for lifespan extension. Since many recent reports demonstrate that both genetic and pharmacological manipulations of the translation machinery can extend longevity in eukaryotes, our study puts lncRNAs forward as a compelling area in the field of aging research.

EXPERIMENTAL PROCEDURES

Nematode Strains

All strains were maintained expanded as previously described (Brenner, 1974). Briefly, nematodes were maintained on NGM OP50 plates at 15°C. The Bristol N2 strain was used as wild-type. Mutant alleles and transgenes used in this study are CB1370 *daf-2(e1370)*, CF1038 *daf-16(mu86)*, CF1515 *daf-16(mu86); daf-2(e1370)*, MQ130 *clk-1(qm30)*, and DA465 *eat-2(ad465)* (obtained from the Caenorhabditis Genetics Center). The extrachromosomal *tts-1*-overexpressing line in Bristol N2 background was huEx645[*Phs::tts-1::SL2::mCherry; Pmyo2::GFP*]. An integrated line was created by irradiation of huEx645[*Phs::tts-1::SL2::mCherry; Pmyo2::GFP*] with 40 Gy using a 137Cs source, and the obtained line was backcrossed two times with the Bristol N2 wild-type strain to generate huIs164[*Phs::tts-1::SL2::mCherry; Pmyo2::GFP*].

Puromycin Treatment

daf-2 nematodes were synchronized and grown on NGM OP50 plates at 15°C until the L4 stage. They were collected and incubated overnight at 25°C in liquid NGM medium including OP50 bacteria, 0.1% Triton X-100, and 50 μg/ml puromycin (Sigma Aldrich).

RNAi

The last exon of *tts-1* was synthesized by Eurofins with BglII and NcoI restriction enzymes sites on the 5′ or 3′ end, respectively, and cloned into the L4440 vector (Addgene) using the same enzymes. This vector was transformed into HT115 *E. coli*. Positive clones were selected by Sanger sequencing and grown overnight at 37°C in Luria broth with 50 μg/ml ampicillin and 0.2 M isopropyl β-D-1-thiogalactopyranoside (IPTG) before seeding.

Synchronization

For experiments, nematodes were synchronized by bleaching and allowed to hatch overnight in M9 buffer (Eisenmann, 2005). The L1 arrested larvae were plated onto NGM OP50 plates or plates inoculated with *tts-1*-specific RNAi bacteria and grown at 15°C until L4 stage, at which point they were shifted to 25°C overnight (for *daf-2*, *daf-2;daf-16*, and controls only).

Lifespan Analysis

Lifespan analysis was performed as previously described (Stout et al., 2013) on 35 mm NGM plates including FUdR (Sigma-Aldrich), 50 μg/ml ampicillin, and 0.2 M IPTG inoculated with the gene-specific siRNA bacteria of interest (Hansen et al., 2005). Lifespan curves and the associated statistics were analyzed using GraphPad Prism software and a Mantel-Haenszel test. The N2 and *daf-2* ± *tts-1* siRNA lifespan curves were performed in biological duplicate.

Peak Calculations

The polysome peak heights and monosomal peak widths were measured from the lower left most point of the peak curve using ImageJ software. Statistics were performed using a Student's t test. The area under the polysome peaks was calculated using R software (http://www.r-project.org/).

Polysome Profiling

Polysome profiling was performed as previously described (Pereboom et al., 2011). The concentration of protein in the lysates was measured with a Bradford reagent (Bio-Rad), and the cytoplasmic ribosome particles were measured by 260 nm optical density readings. Either an equal amount of total protein or equal levels of cytoplasmic rRNA were loaded onto the sucrose gradients for every experiment. Fractions were collected using a Foxy Jr Fraction Collector (Teledyne ISCO).

RNA-Sequencing Analysis

Monosomal and polysomal fractions from two experiments were pooled and RNA was extracted using TRIzol LS (Invitrogen) according to the manufacturer's protocol. For each condition, two libraries were constructed from RNA isolated from two separate experiments using the SOLiD Total RNA-Seq Kit (Life Technologies) and analyzed on the SOLiD platform. The sequence reads were mapped against the genome assembly WBcel215. Using cufflinks,

we identified any possible new transcripts through reference annotated base transcript (RABT) assembly (Trapnell et al., 2013). Subsequently differential expression of transcripts was determined using cuffdiff across all pairs (Trapnell et al., 2013).

GO Term Cluster Analysis
GO analysis was performed by DAVID analysis (Huang et al., 2009a, 2009b).

qPCR Analysis
Total, monosomal, and polysomal RNA was isolated using TRIzol LS (Invitrogen) according to manufacturer's protocol, and cDNA was made using iScript (Bio-Rad). qPCR reactions were run using iQ SYBR Green Supermix (Bio-Rad) on a myIQ iCycler (Bio-Rad), and the expression of the RNAs were calculated using the ΔCt method. The following primers were used for total RNA measurements: *tts-1* forward (fw): 5′-CCGACACGTTTCAGACACAC-3′, *tts-1* reverse (rv): 5′-G GTTTTACCCATTGACTCAACC-3′, *pmp-3* fw: 5′-TCCTTGATGAATCCACGT CA-3′, and *pmp-3* rv: 5′-ACCGATGACCAATTGACACA-3′. For mono- and polysomal RNA, *tts-1* fw: 5′-ACCTAACTTGCCTGCTTCCA-3′ and *tts-1* rev: 5′-CG GAGGATTGAGGAAAATTG-3′. For 18S rRNA, fw: 5′-TTGCTGCGGTTAAAAA GCTC-3′ and rev: 5′-CCAACCTCAAACCAGCAAAT-3′. For the rRNA qPCR, the cDNA was diluted 1:1,000 and the final calculation multiplied by 1,000. All statistical analysis was performed with a Student's t test.

Fluorescent In Situ Hybridization
A set of 11 short probes targeting *tts-1* was designed with the Stellaris RNA FISH probe designer, using the highest level of masking (BioSearch Technologies). The probe sequences are as follows: #1: 5′-AGTCATAAGAAAAA AACTCG-3′; #2: 5′-CGATATGGAACTCAATTTCC-3′, #3: 5′-GCGAAAAGAT ATTTATACCG-3′, #4: 5′-TAAGGTCTTTTGAACTGGCC-3′, #5: 5′-GTTGGTAC ACTGAAGACTGT-3′, #6: 5′-CCGTGTCCTTGGGACATTGT-3′, #7: 5′-AGA GCTGAAGAGCATTTACC-3′, #8: 5′-CGTGAAGAAGTTTACGAGAC-3′, #9: 5′-TGCGAAAAAGACTACTACCA-3′, #10: 5′-CTGCTGCCCAAAAACTATGT-3′, #11: 5′-ACTCAGTTACCCATTTTGGA-3′. FISH was performed according to the manufacturers' protocol with the following modifications: nematodes were hybridized in a 1,250 μM probe solution overnight at 37°C, washed once for 8 hr, once overnight, and finally for 1 hr in the presence of DAPI before imaging on a DM6000 microscope (Leica Microsystems). Images were processed using ImageJ V1.46r.

ACCESSION NUMBERS

The next-generation sequencing data reported in this paper have been deposited to the European Nucleotide Archive and are available under accession number PRJEB8029.

SUPPLEMENTAL INFORMATION

Supplemental Information includes four figures and two tables and can be found with this article online at http://dx.doi.org/10.1016/j.celrep.2014.12.029.

AUTHOR CONTRIBUTIONS

P.B.E., J.N., and Y.J.G. performed most of the experiments with the help of B.M. and M.V. N.L. performed the next-generation sequencing. R.J. performed the bioinformatics analysis. The *C. elegans* experiments were performed in the lab of H.C.K. under the guidance of M.C.B. A.B.B. designed experiments and interpreted results. A.W.M. conceived the project, designed experiments, interpreted results, and wrote the manuscript.

ACKNOWLEDGMENTS

REFERENCES

Apfeld, J., O'Connor, G., McDonagh, T., DiStefano, P.S., and Curtis, R. (2004). The AMP-activated protein kinase AAK-2 links energy levels and insulin-like signals to lifespan in C. elegans. Genes Dev. *18*, 3004–3009.

Blagosklonny, M.V. (2010). Calorie restriction: decelerating mTOR-driven aging from cells to organisms (including humans). Cell Cycle *9*, 683–688.

Brenner, S. (1974). The genetics of Caenorhabditis elegans. Genetics *77*, 71–94.

Curtis, R., O'Connor, G., and DiStefano, P.S. (2006). Aging networks in Caenorhabditis elegans: AMP-activated protein kinase (aak-2) links multiple aging and metabolism pathways. Aging Cell *5*, 119–126.

Depuydt, G., Xie, F., Petyuk, V.A., Smolders, A., Brewer, H.M., Camp, D.G., 2nd, Smith, R.D., and Braeckman, B.P. (2014). LC-MS proteomics analysis of the insulin/IGF-1-deficient Caenorhabditis elegans daf-2(e1370) mutant reveals extensive restructuring of intermediary metabolism. J. Proteome Res. *13*, 1938–1956.

Eisenmann, D.M., ed. (2005). *WormBook*. The *C. elegans* Research Community. 10.1895/wormbook.1.7.1, http://www.wormbook.org.

Guttman, M., Russell, P., Ingolia, N.T., Weissman, J.S., and Lander, E.S. (2013). Ribosome profiling provides evidence that large noncoding RNAs do not encode proteins. Cell *154*, 240–251.

Halaschek-Wiener, J., Khattra, J.S., McKay, S., Pouzyrev, A., Stott, J.M., Yang, G.S., Holt, R.A., Jones, S.J., Marra, M.A., Brooks-Wilson, A.R., and Riddle, D.L. (2005). Analysis of long-lived C. elegans daf-2 mutants using serial analysis of gene expression. Genome Res. *15*, 603–615.

Hansen, M., Hsu, A.L., Dillin, A., and Kenyon, C. (2005). New genes tied to endocrine, metabolic, and dietary regulation of lifespan from a Caenorhabditis elegans genomic RNAi screen. PLoS Genet. *1*, 119–128.

Hansen, M., Taubert, S., Crawford, D., Libina, N., Lee, S.J., and Kenyon, C. (2007). Lifespan extension by conditions that inhibit translation in Caenorhabditis elegans. Aging Cell *6*, 95–110.

Hardie, D.G. (2011). AMP-activated protein kinase: an energy sensor that regulates all aspects of cell function. Genes Dev. *25*, 1895–1908.

Houtkooper, R.H., Mouchiroud, L., Ryu, D., Moullan, N., Katsyuba, E., Knott, G., Williams, R.W., and Auwerx, J. (2013). Mitonuclear protein imbalance as a conserved longevity mechanism. Nature *497*, 451–457.

Huang, W., Sherman, B.T., and Lempicki, R.A. (2009a). Bioinformatics enrichment tools: paths toward the comprehensive functional analysis of large gene lists. Nucleic Acids Res. *37*, 1–13.

Huang, W., Sherman, B.T., and Lempicki, R.A. (2009b). Systematic and integrative analysis of large gene lists using DAVID bioinformatics resources. Nat. Protoc. *4*, 44–57.

Ivanov, P., Emara, M.M., Villen, J., Gygi, S.P., and Anderson, P. (2011). Angiogenin-induced tRNA fragments inhibit translation initiation. Mol. Cell *43*, 613–623.

Jonassen, T., Proft, M., Randez-Gil, F., Schultz, J.R., Marbois, B.N., Entian, K.D., and Clarke, C.F. (1998). Yeast Clk-1 homologue (Coq7/Cat5) is a mitochondrial protein in coenzyme Q synthesis. J. Biol. Chem. *273*, 3351–3357.

Jones, S.J., Riddle, D.L., Pouzyrev, A.T., Velculescu, V.E., Hillier, L., Eddy, S.R., Stricklin, S.L., Baillie, D.L., Waterston, R., and Marra, M.A. (2001). Changes in gene expression associated with developmental arrest and longevity in Caenorhabditis elegans. Genome Res. *11*, 1346–1352.

Kamath, R.S., Martinez-Campos, M., Zipperlen, P., Fraser, A.G., and Ahringer, J. (2001). Effectiveness of specific RNA-mediated interference through ingested double-stranded RNA in Caenorhabditis elegans. Genome Biol. *2*, H0002.

Kamath, R.S., Fraser, A.G., Dong, Y., Poulin, G., Durbin, R., Gotta, M., Kanapin, A., Le Bot, N., Moreno, S., Sohrmann, M., et al. (2003). Systematic functional analysis of the Caenorhabditis elegans genome using RNAi. Nature *421*, 231–237.

Kenyon, C.J. (2010). The genetics of ageing. Nature *464*, 504–512.

Kenyon, C., Chang, J., Gensch, E., Rudner, A., and Tabtiang, R. (1993). A C. elegans mutant that lives twice as long as wild type. Nature *366*, 461–464.

Lakowski, B., and Hekimi, S. (1996). Determination of life-span in Caenorhabditis elegans by four clock genes. Science *272*, 1010–1013.

Lakowski, B., and Hekimi, S. (1998). The genetics of caloric restriction in Caenorhabditis elegans. Proc. Natl. Acad. Sci. USA *95*, 13091–13096.

Libina, N., Berman, J.R., and Kenyon, C. (2003). Tissue-specific activities of C. elegans DAF-16 in the regulation of lifespan. Cell *115*, 489–502.

Mair, W., Morantte, I., Rodrigues, A.P., Manning, G., Montminy, M., Shaw, R.J., and Dillin, A. (2011). Lifespan extension induced by AMPK and calcineurin is mediated by CRTC-1 and CREB. Nature *470*, 404–408.

McElwee, J., Bubb, K., and Thomas, J.H. (2003). Transcriptional outputs of the Caenorhabditis elegans forkhead protein DAF-16. Aging Cell *2*, 111–121.

Meléndez, A., Tallóczy, Z., Seaman, M., Eskelinen, E.L., Hall, D.H., and Levine, B. (2003). Autophagy genes are essential for dauer development and life-span extension in C. elegans. Science *301*, 1387–1391.

Murphy, C.T. (2006). The search for DAF-16/FOXO transcriptional targets: approaches and discoveries. Exp. Gerontol. *41*, 910–921.

Murphy, C.T., McCarroll, S.A., Bargmann, C.I., Fraser, A., Kamath, R.S., Ahringer, J., Li, H., and Kenyon, C. (2003). Genes that act downstream of DAF-16 to influence the lifespan of Caenorhabditis elegans. Nature *424*, 277–283.

Niazi, F., and Valadkhan, S. (2012). Computational analysis of functional long noncoding RNAs reveals lack of peptide-coding capacity and parallels with 3′ UTRs. RNA *18*, 825–843.

O'Rourke, D., Baban, D., Demidova, M., Mott, R., and Hodgkin, J. (2006). Genomic clusters, putative pathogen recognition molecules, and antimicrobial genes are induced by infection of C. elegans with M. nematophilum. Genome Res. *16*, 1005–1016.

Pereboom, T.C., van Weele, L.J., Bondt, A., and MacInnes, A.W. (2011). A zebrafish model of dyskeratosis congenita reveals hematopoietic stem cell formation failure resulting from ribosomal protein-mediated p53 stabilization. Blood *118*, 5458–5465.

Pircher, A., Bakowska-Zywicka, K., Schneider, L., Zywicki, M., and Polacek, N. (2014). An mRNA-derived noncoding RNA targets and regulates the ribosome. Mol. Cell *54*, 147–155.

Robinson, J.T., Thorvaldsdóttir, H., Winckler, W., Guttman, M., Lander, E.S., Getz, G., and Mesirov, J.P. (2011). Integrative genomics viewer. Nat. Biotechnol. *29*, 24–26.

Smith, J.E., Alvarez-Dominguez, J.R., Kline, N., Huynh, N.J., Geisler, S., Hu, W., Coller, J., and Baker, K.E. (2014). Translation of small open reading frames within unannotated RNA transcripts in Saccharomyces cerevisiae. Cell Rep. *7*, 1858–1866.

Sobala, A., and Hutvagner, G. (2013). Small RNAs derived from the 5′ end of tRNA can inhibit protein translation in human cells. RNA Biol. *10*, 553–563.

Steffen, K.K., MacKay, V.L., Kerr, E.O., Tsuchiya, M., Hu, D., Fox, L.A., Dang, N., Johnston, E.D., Oakes, J.A., Tchao, B.N., et al. (2008). Yeast life span extension by depletion of 60s ribosomal subunits is mediated by Gcn4. Cell *133*, 292–302.

Stout, G.J., Stigter, E.C., Essers, P.B., Mulder, K.W., Kolkman, A., Snijders, D.S., van den Broek, N.J., Betist, M.C., Korswagen, H.C., Macinnes, A.W., and Brenkman, A.B. (2013). Insulin/IGF-1-mediated longevity is marked by reduced protein metabolism. Mol. Syst. Biol. *9*, 679.

Trapnell, C., Hendrickson, D.G., Sauvageau, M., Goff, L., Rinn, J.L., and Pachter, L. (2013). Differential analysis of gene regulation at transcript resolution with RNA-seq. Nat. Biotechnol. *31*, 46–53.

van Heesch, S., van Iterson, M., Jacobi, J., Boymans, S., Essers, P.B., de Bruijn, E., Hao, W., MacInnes, A.W., Cuppen, E., and Simonis, M. (2014). Extensive localization of long noncoding RNAs to the cytosol and mono- and polyribosomal complexes. Genome Biol. *15*, R6.

Wilson, B.A., and Masel, J. (2011). Putatively noncoding transcripts show extensive association with ribosomes. Genome Biol. Evol. *3*, 1245–1252.

Wong, A., Boutis, P., and Hekimi, S. (1995). Mutations in the clk-1 gene of Caenorhabditis elegans affect developmental and behavioral timing. Genetics *139*, 1247–1259.

Yoon, J.H., Abdelmohsen, K., Srikantan, S., Yang, X., Martindale, J.L., De, S., Huarte, M., Zhan, M., Becker, K.G., and Gorospe, M. (2012). LincRNA-p21 suppresses target mRNA translation. Mol. Cell *47*, 648–655.

Zhang, Y., Chen, D., Smith, M.A., Zhang, B., and Pan, X. (2012). Selection of reliable reference genes in Caenorhabditis elegans for analysis of nanotoxicity. PLoS ONE *7*, e31849.
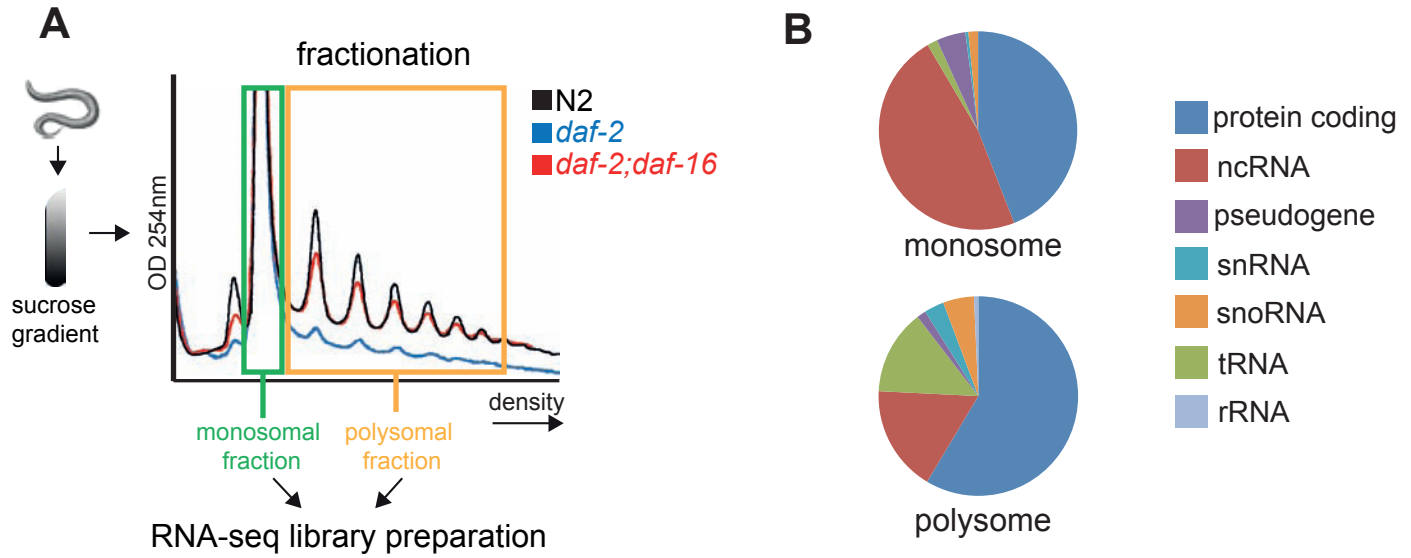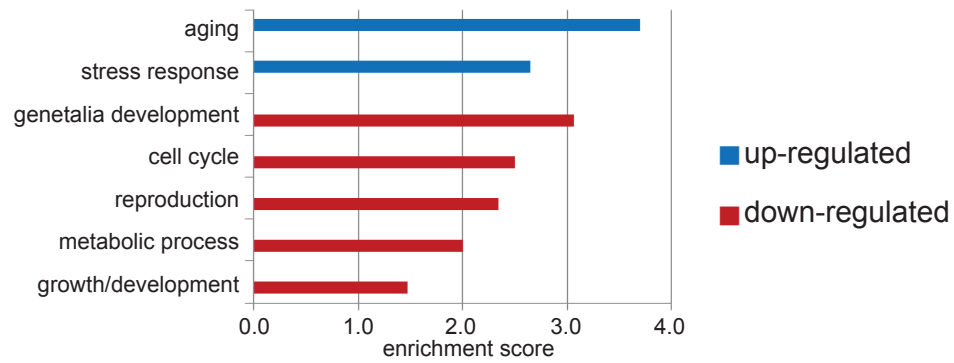
A Long Noncoding RNA on the Ribosome

Is Required for Lifespan Extension

Paul B. Essers, Julie Nonnekens, Yvonne J. Goos, Marco C. Betist, Marjon D. Viester, Britt Mossink, Nico Lansu, Hendrik C. Korswagen, Rob Jelier, Arjan B. Brenkman, and Alyson W. MacInnes
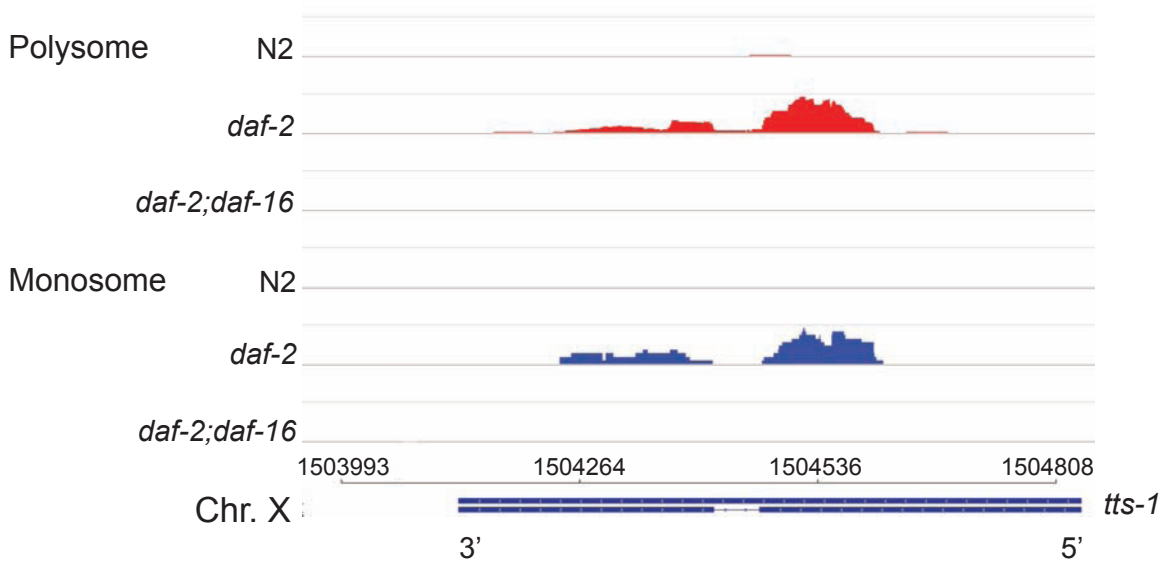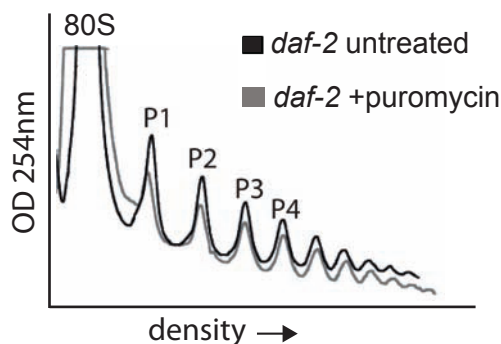
Figure S1
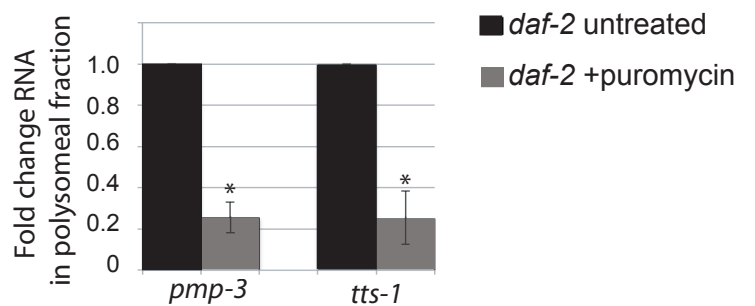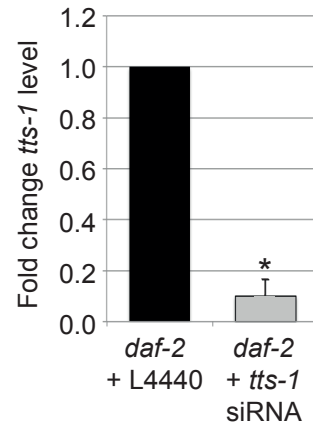
Figure S2

A

B

				Longevity (days)			
Strain	Vector/target	RNAi from	Temp (°C)	median	maximum	# nematodes	*p*- value to N2 + L4440
N2	L4440	L4	25	14	18	160	-
N2	*tts-1*	L4	25	12	18	125	0.5454

				Longevity (days)			
Strain	Vector/target	RNAi from	Temp (°C)	median	maximum	# nematodes	*p*- value to *daf-2* + L4440
daf-2	L4440	L4	25	39	47	114	-
daf-2	*tts-1*	L4	25	28	47	127	< 0.0001
daf-2	*daf-16*	L4	25	18	29	93	< 0.0001
daf-2;16	L4440	L4	25	9	14	112	<0.0001
daf-2;16	L4440	L4	25	9	14	153	<0.0001

				Longevity (days)			
Strain	Vector/target	RNAi from	Temp (°C)	median	maximum	# nematodes	*p*- value to *daf-2;16* + L4440
daf-2;16	L4440	L4	25	9	14	112	-
daf-2;16	L4440	L4	25	9	14	153	0.1902

Figure S3

A

B

Figure S4

A

B

C
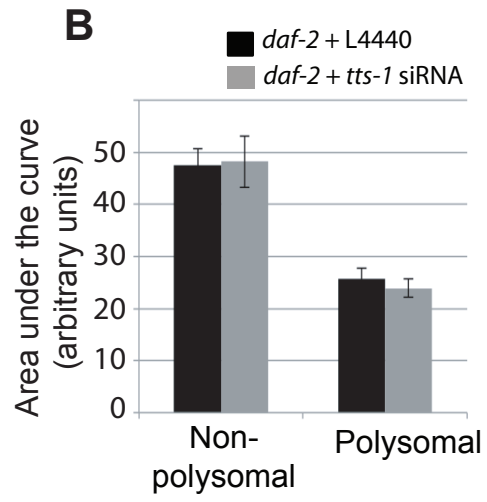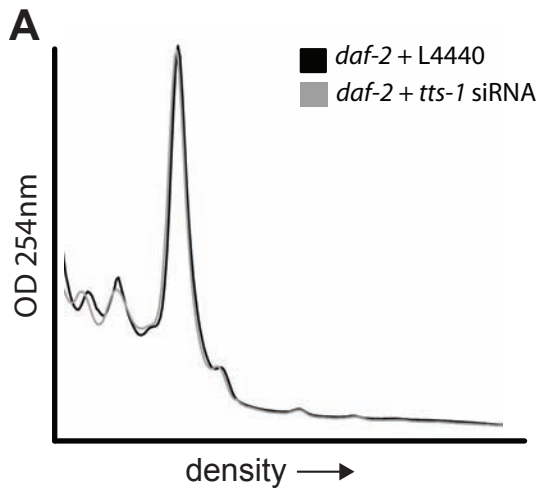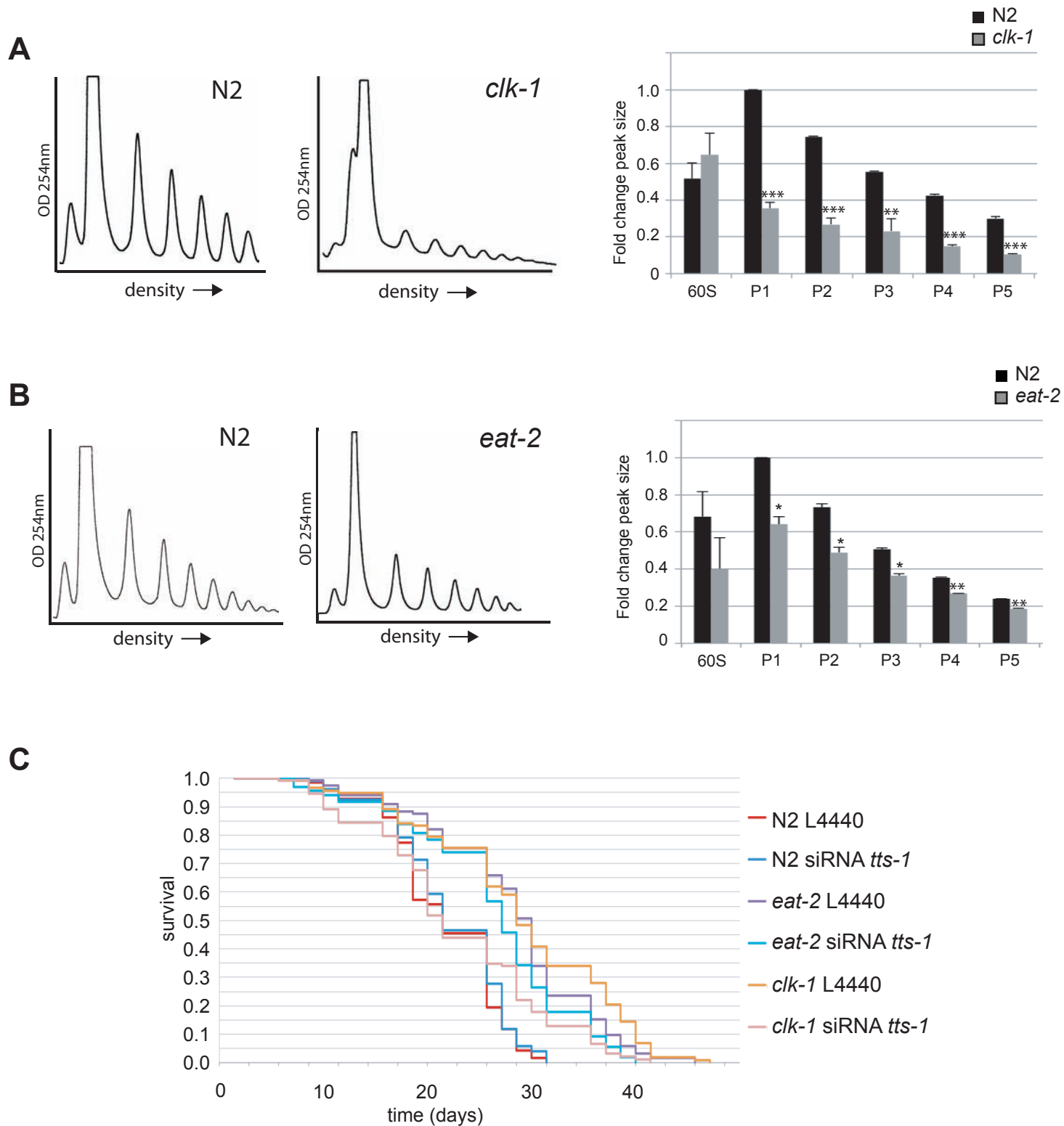
D

			Longevity (days)			
strain	vector/target	temp	median	maximum	# nematodes	*p*-value to N2 +L4440
N2	L4440	25	15	22	135	-
N2	*tts-1*	25	15	22	111	0.35

			Longevity (days)			
strain	vector/target	temp	median	maximum	# nematodes	*p*-value to *clk-1* +L4440
clk-1	L4440	25	20	33	119	-
clk-1	*tts-1*	25	15	29	126	>0.0001

			Longevity (days)			
strain	vector/target	temp	median	maximum	# nematodes	*p*-value to *eat-2* +L4440
eat-2	L4440	25	21	32	165	-
eat-2	*tts-1*	25	19	28	137	0.0206

Figure S1, Related to Figure 1.

A) The experimental set-up where *C. elegans* strains are lysed and cushioned on sucrose gradients for polysome fractionation. The monosomal and pooled polysomal peaks are isolated for purification of RNAs used to prepare next-generation RNA sequencing libraries. The representative peak sizes are shown. B) The relative proportion of the different RNAs found by next-generation sequencing of monosomal or polysomal fractions in all three strains, N2, *daf-2*, and *daf-2;daf-16.* C) The enrichment score of GO-terms determined by DAVID analysis comparing the gene functions of N2 vs. *daf-2* mRNAs found in the monosomal fraction. Blue = up-regulated in *daf-2*, red = down-regulated in *daf-2*. D) Mapped read density of the *tts-1* gene for the three genetic backgrounds, both monosome and polysome fractions. Read depth is indicated. Below the two annotated *tts-1* gene structures are shown on their position on Chromosome X. E) Representative polysome profiles of *daf-2* mutants (black line) vs. *daf-2* mutants treated with puromycin overnight (grey line). F) The fold change of *pmp-3* and *tts-1* levels in the polysomal fractions of *daf-2* mutants treated or untreated with puromycin, measured by qPCR analysis. *p<0.01.

Figure S2, Related to Figure 2.

A) qPCR analysis of *tts-1* levels in *daf-2* mutants either fed bacteria transformed with L4440 (black) or L4440 expressing an siRNA against *tts-1* (grey). *p<0.01. B) Statistical analysis of the longevity curves in Figure 2.

Figure S3, Related to Figure 3.

A) Representative polysome profiles of *daf-2* mutants either fed bacteria transformed with L4440 (black line) or L4440 expressing an siRNA against *tts-1* (grey line) when cell lysates are normalized to cytoplasmic rRNA levels. B) Measurements of the areas under the polysomal peaks vs. the non-polysomal peaks.

Figure S4, Related to Figure 4.

A) Representative polysome profiles of N2 compared to *clk-1* mutants and the quantification of their peak sizes. B) Polysome profiles of N2 compared to *eat-2* mutants and the quantification of their peak sizes. $*p<0.02$, $**p<0.005$, $***p<0.001$. C) The survival curves of N2, *clk-1,* and *eat-2* strains fed bacteria expressing empty L4440 vector or L4440 expressing the siRNA against *tts-1.* D) Statistical analysis of the longevity assay in Figure 4.

Table S1. Next-generation sequencing results comparing monosomal RNAs from N2, *daf-2,* and *daf-2;daf-16* strains.

Table S2. Next-generation sequencing results comparing polysomal RNAs from N2, *daf-2,* and *daf-2;daf-16* strains.